ACS APPLIED MATERIALS & INTERFACES

Research Article

www.acsami.org

Surface Passivation Effect on the Photoluminescence of ZnO Nanorods

Cong Chen, Haiping He, Yangfan Lu,* Kewei Wu, and Zhizhen Ye

State Key Laboratory of Silicon Materials, Department of Materials Science and Engineering, Zhejiang University, Hangzhou 310027, People's Republic of China

ABSTRACT: We report an investigation of the impact of surface passivation on the optical properties of ZnO nanorods. Al_2O_3 coating and hydrogen plasma treatment were used to passivate the surface states. It was found that Al_2O_3 coating led to the suppression of the deep level emissions, while hydrogen plasma treatment completely quenched the deep level emissions. It was confirmed that the surface states of the as-grown ZnO nanorod arrays indeed contributed to the deep level emissions. Evidence was also provided that shows surface states have a greater impact on the green emission than the orange emission and may cause the negative thermal quenching behavior. Moreover, the passivation effect was confirmed by the changes of the O 1s and Zn 2p spectra.

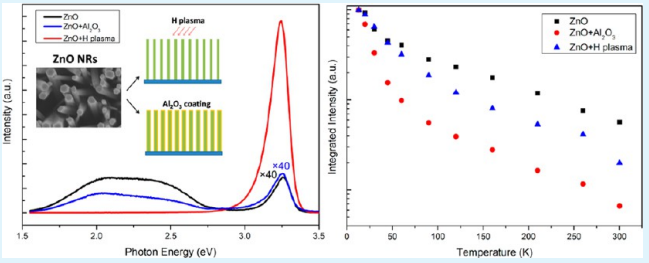

KEYWORDS: *ZnO nanorods, Al_2O_3 coating, hydrogen plasma, photoluminescence, surface passivation*

INTRODUCTION

One-dimensional ZnO structures, which exhibit excellent electrical and optical properties, have attracted extensive attention because of their potential applications in optoelectronics.[1] Photoluminescence (PL) of ZnO nanostructures have been widely studied in recent years.[2] Because of the large surface-to-volume ratio, surface states play important roles on the PL properties of ZnO nanostructures and thus surface state-related excitonic emissions (SX) in ZnO nanostructures have been frequently observed.[3] In addition, green emission is commonly observed in ZnO nanostructures and many researchers think that surface states are responsible for the green emission.[4] However, some different hypotheses have been proposed that bulk defects such as oxygen vacancies are also responsible for the green emission.[5]

Moreover, many researchers tailored the optical properties of ZnO nanostructures through surface modification.[5−7] Richters et al.[5] have studied the PL properties of ZnO/Al_2O_3 core−shell nanowires. They found that the near band emission (NBE) at low temperature was enhanced, whereas the deep level emissions at room temperature were reduced. In addition, hydrogenation can also improve PL by both decreasing the deep level emissions and increasing the NBE.[7] Other surface treatment methods such as polymer covering[8] and argon ion milling[9] have also been demonstrated to suppress the deep level emissions while enhancing the ultraviolet (UV) emission of ZnO. These surface treatment methods may help us study the impact of surface states on the optical properties of ZnO nanostructures and provide new insights to understand the surface passivation mechanism.

Al_2O_3 coating and hydrogen plasma treatment were used to discuss the impact of surface states on the optical properties of ZnO. Temperature-dependent PL of the as-grown, Al_2O_3-coated and H plasma treated ZnO nanorod arrays was investigated. It can be seen that Al_2O_3 coating leads to the suppression of the deep level emissions while H plasma treatment completely quenches the deep level emissions. The results indicate that surface states have a great impact on the green emission of the as-grown sample than the orange emission. The present results can promote our understanding of the optical properties of ZnO nanostructures.

EXPERIMENTAL SECTION

The ZnO nanorod arrays were grown on a Si (100) substrate using the hydrothermal method by two steps. First, 100 nm thick ZnO seed layers were deposited on the Si(100) substrate by radio frequency magnetron sputtering from a ZnO target at 450 °C with the sputtering power kept at 150 W and the deposition time set at 30 min. Then the substrate was immersed into the aqueous solution containing 20 mM zinc nitrate hydrate and 4 mL ammonia and heated to 70 °C for 12h. After the growth, the substrate was washed by deionized water and dried by N_2. Then the samples were placed in a vacuumed chamber at 200 °C for 1 h to eliminate the absorbed hydroxyl groups. Figure 1a shows the morphology of the synthesized ZnO nanorod arrays with average diameter of ∼200 nm, which which exhibit smooth surfaces.

The Al_2O_3 thin films were deposited on as-grown ZnO nanorod arrays via Thermal ALD using a showerhead-type ALD system (KJLC 150LX). Trimethylaluminium (TMA, 99.999%) precursor was used for the deposition of Al_2O_3. The carrier gas and purging medium were 99.999% purity argon. During the growth, the pressure in the chamber was ∼1.5 Torr, and the substrate temperature was held at 150 °C. A typical Al_2O_3 growth sequence was composed of 0.1 s of TMA

Received: April 18, 2013
Accepted: June 10, 2013
Published: June 10, 2013

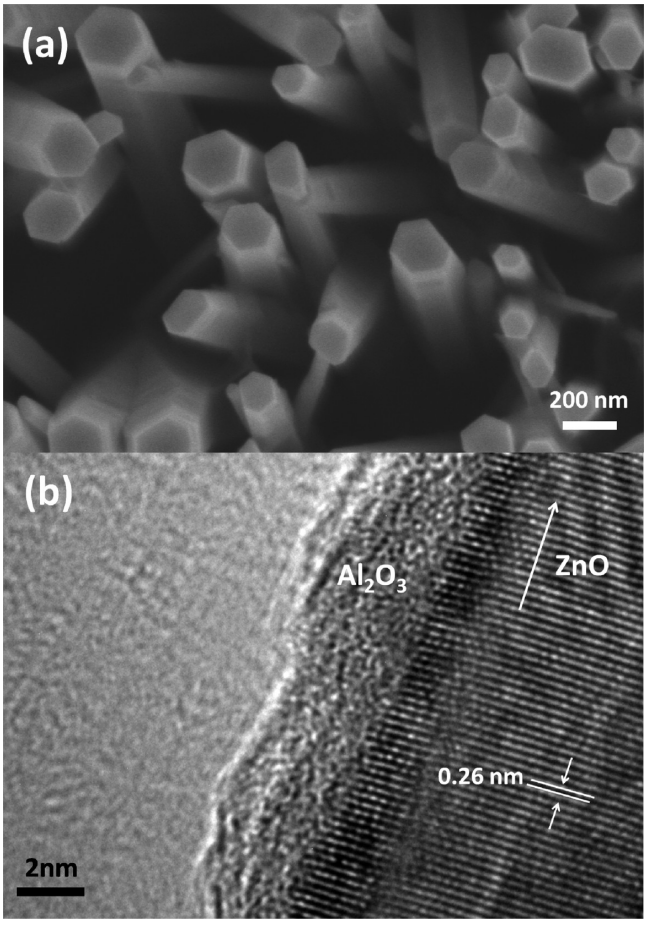

Figure 1. (a) SEM image of the as-grown ZnO nanorods. (b) HRTEM image of the ZnO nanorod coated with Al_2O_3 layer.

exposure, 5 s of Ar purging, 0.1 s of H_2O exposure, and 10 s of Ar purging. The growth rate of Al_2O_3 was about 0.1 nm/cycle. Figure 1b shows that the ZnO nanorod is coated by the Al_2O_3 shell with a thickness of ~3 nm.

The hydrogen (H) plasma treatments for the as-grown ZnO nanorod arrays were performed in dc plasma for 40 min at room temperature. The plasma power was set at 20 W and the pressure was set at 10 mTorr. The morphology of the ZnO nanorod arrays does not change much after H plasma treatment (not shown here).

The morphology of the samples was characterized by a field emission scanning electron microscopy (FESEM, Hitachi S4800) and a high-resolution transmission electron microscope (HRTEM, Tecnai G2 F30 S-Twin). PL spectra were recorded using a FLS920 fluorescence spectrometer (Edinburgh Instruments) with a 325 nm He−Cd Laser as excitation source equipped with a variable attenuator. PL measurements were conducted at temperatures ranging from 13 to 300 K. The changes of chemical states on the surface of ZnO after surface treatments were recorded by the X-ray photoelectron spectroscopy (XPS). The measurements were conducted on a Thermo ESCALAB 250 system with a monochromatic Al−Kα ($h\nu$ = 1486.6 eV) X-ray source.

RESULTS AND DISCUSSION

The room-temperature PL spectra of the as-grown ZnO nanorod arrays presents a near band emission (NBE) around 3.24 eV and a broad visible emission that is usually attributed to defect emission, as shown in Figure 2a. It has been known that the NBE of ZnO at room temperature is attributed to the free-exciton recombination and its longitudinal-optical phonon replica. However, there is no consensus on the photo-

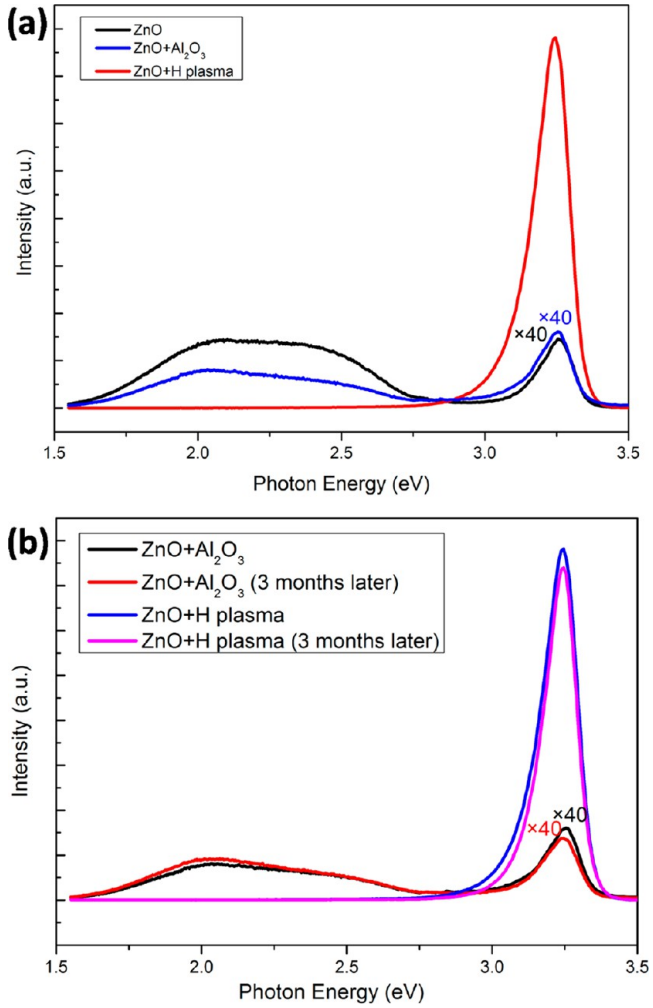

Figure 2. (a) Room-temperature PL spectra of the as-grown, Al_2O_3 coated and H plasma-treated ZnO nanorods. (b) Room-temperature PL spectra of the Al_2O_3 coated and H plasma-treated samples before and after exposure to ambient air for 3 months.

luminescence mechanism of the visible emission. Many researchers have suggested that the visible emission is attributed to the oxygen vacancies.[10] It have been also proposed that Cu impurities are responsible for the visible emission.[11] Some researchers also considered that surface states of ZnO nanostructures can contribute to the visible emission.[4] After Al_2O_3 coating, it is found that the NBE is little affected by the coating and the visible emission is partially suppressed. Surface states such as surface adsorption and dangling bonds, can be passivated by Al_2O_3 coating,[12] leading to the suppression of the deep level emissions caused by surface states. Moreover, the oxygen vacancies on the surface can be passivated by coating of oxides. In our experiments, the suppression of deep level emissions can also be attributed to surface passivation model. It also gives evidence that the surface states of the as-grown ZnO nanorod arrays indeed contribute to the deep level emissions, whereas the visible emission of H plasma-treated ZnO is completely quenched and the NBE is greatly enhanced by ~100 times compared with that of the as-grown ZnO. The nonradiative recombination centers can be passivated by H, resulting in the enhancement of the NBE of ZnO. Similar observations for the passivation by H plasma treatment on ZnO were also reported.[13] Moreover, additional radiative recombi-

dx.doi.org/10.1021/am401418b | ACS Appl. Mater. Interfaces 2013, 5, 6354−6359

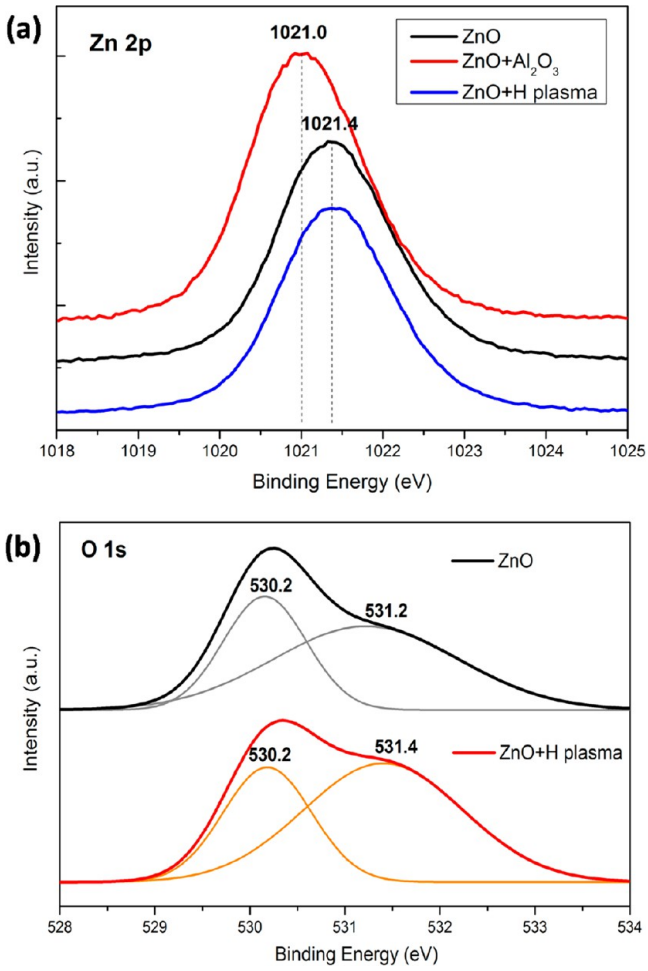

Figure 3. XPS spectra corresponding to (a) Zn 2p and (b) O 1s peaks of the as-grown, Al_2O_3 coated and H plasma treated ZnO nanorods.

nation emission can be caused by H doping,[14] which would contribute to the NBE. Huang et al.[15,16] have also observed the PL evolution that the visible emission was quenched and the NBE was enhanced after annealing. They attributed the enhancement of NBE to hydrogen doping by directly probing with solid state nuclear magnetic resonance. Thus in our work, both surface passivation effect and hydrogen doping are responsible for the change of PL. Therefore, the NBE is greatly enhanced and the visible emission is completely suppressed after H plasma treatment. The Al_2O_3-coated and H-plasma treated samples were exposed to ambient air for 3 months to evaluate their stability. Figure 2b reveals the PL spectra of the Al_2O_3-coated and H plasma-treated samples before and after exposure, showing only slight changes induced by surface adsorption. Thus the ZnO nanorods show good stability of PL after these surface treatments.

XPS measurements were used to determine the changes of chemical states on the surface of ZnO after surface treatments. Figure 3a shows Zn $2p_{2/3}$ lines of the as-grown, Al_2O_3-coated, and H plasma-treated samples. A Zn $2p_{2/3}$ peak at 1021.4 eV is observed in the as-grown nanorods. After coating, the peak shifts to 1021.0 eV. The 0.4 eV shifting shows that the chemical state of Zn is changed because dangling bonds such as Zn- may be passivated by O after Al_2O_3 coating. Two distinct peaks are observed in the O 1s core level spectra of the as-grown and H plasma-treated samples. Although the peak at the binding

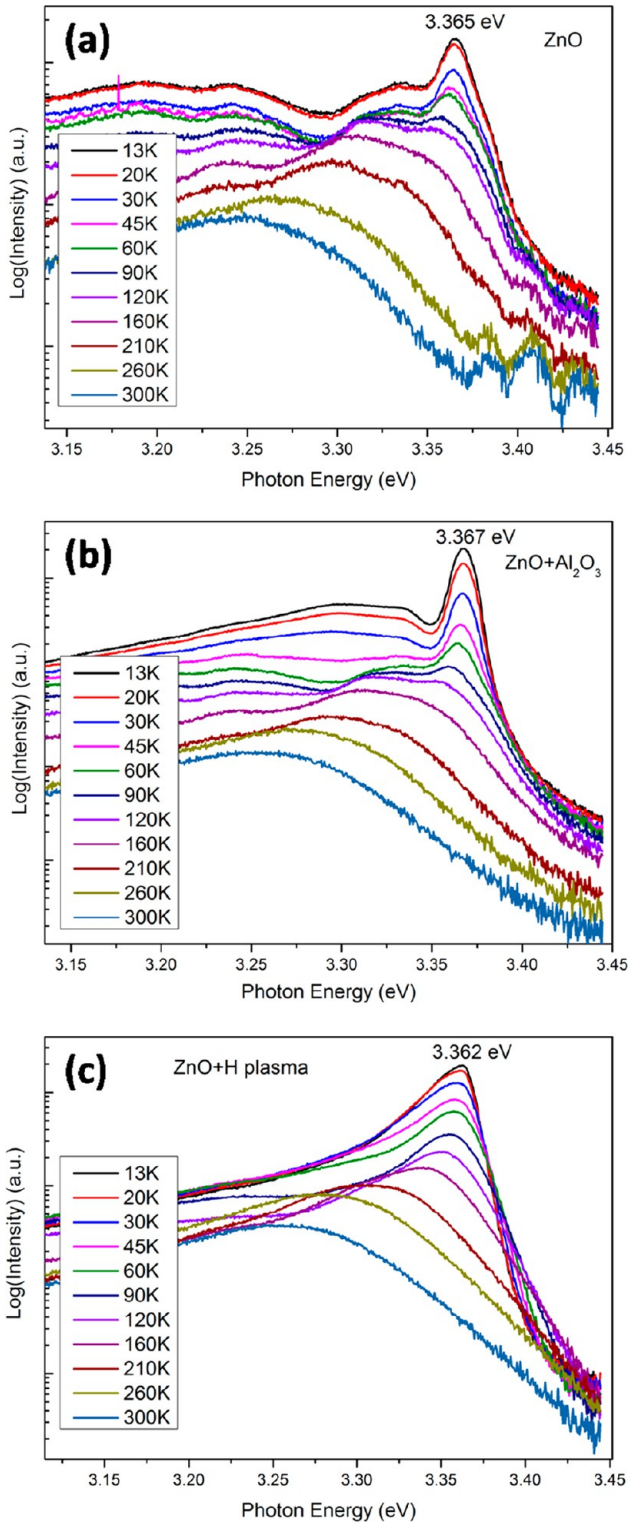

Figure 4. Temperature-dependent PL spectra of the (a) as-grown, (b) Al_2O_3-coated and (c) H plasma-treated ZnO nanorods.

energy of 530.2 eV is a characteristic value reported for Zn−O−Zn,[17] the peaks at the binding energy of 531.2 and 531.4 eV could be attributed to V_O or Zn−O−H. Their binding energies are typically slightly higher than the value reported for Zn−O−Zn.[18,19] According to the Gaussian fitting results, H plasma treated sample shows a much stronger peak at 531.4 eV compared with the as-grown sample, indicating an increased

dx.doi.org/10.1021/am401418b | ACS Appl. Mater. Interfaces 2013, 5, 6354−6359

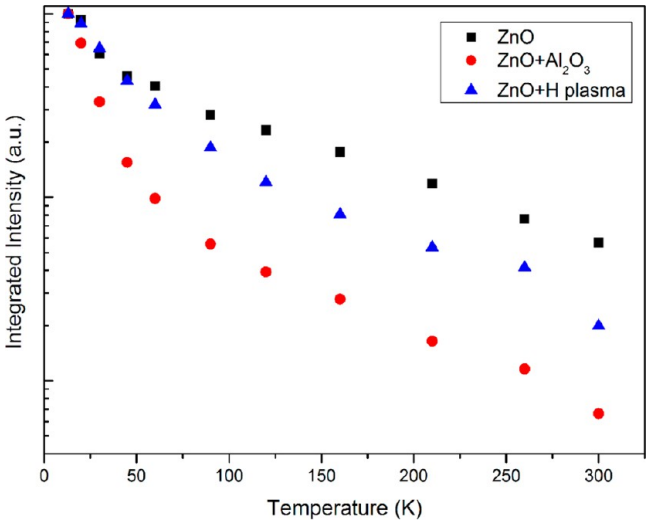

Figure 5. Normalized PL intensity of the excitonic emission as a function of temperature for the as-grown, Al_2O_3-coated, and H plasma-treated samples.

density of hydroxyl groups and V_O on the surface. It gives evidence that dangling bonds such as O− can be passivated by H. The XPS results here confirm the surface passivation effect by surface treatment.

Figure 4 shows the temperature-dependent PL spectra of the NBE of the samples (as-grown, Al_2O_3-coated, and H plasma-treated). A dominant excitonic line at 3.365 eV at 13 K is observed in the as-grown ZnO. We now attribute it as the neutral donor bound excition emission (D^0X). With the increasing temperature, it gradually transforms into free exciton emission and the PL intensity decreases monotonically, which is a characteristic of normal thermal behavior. The Al_2O_3-coated sample shows a dominant excitonic line at 3.367 eV while the H plasma treated sample shows a dominant excitonic line at 3.362 eV. The peak at 3.362 eV is in agreement with the reported transition energy of excitons bound to hydrogen.[20] Figure 5 shows the normalized integrated PL intensity of the samples at temperatures ranging from 13 to 300 K. Compared with the as-grown ZnO, the PL intensities of the Al_2O_3-coated and H plasma-treated samples decay more quickly with increasing temperature. We explain this phenomenon by the surface band bending model. For the as-grown ZnO nanorods, surface defects and the surface adsorption will trap free electrons and generate upward band bending near the surface. Thus the photogenerated carriers can be separated and the photogenerated holes accumulate near the surface, which will

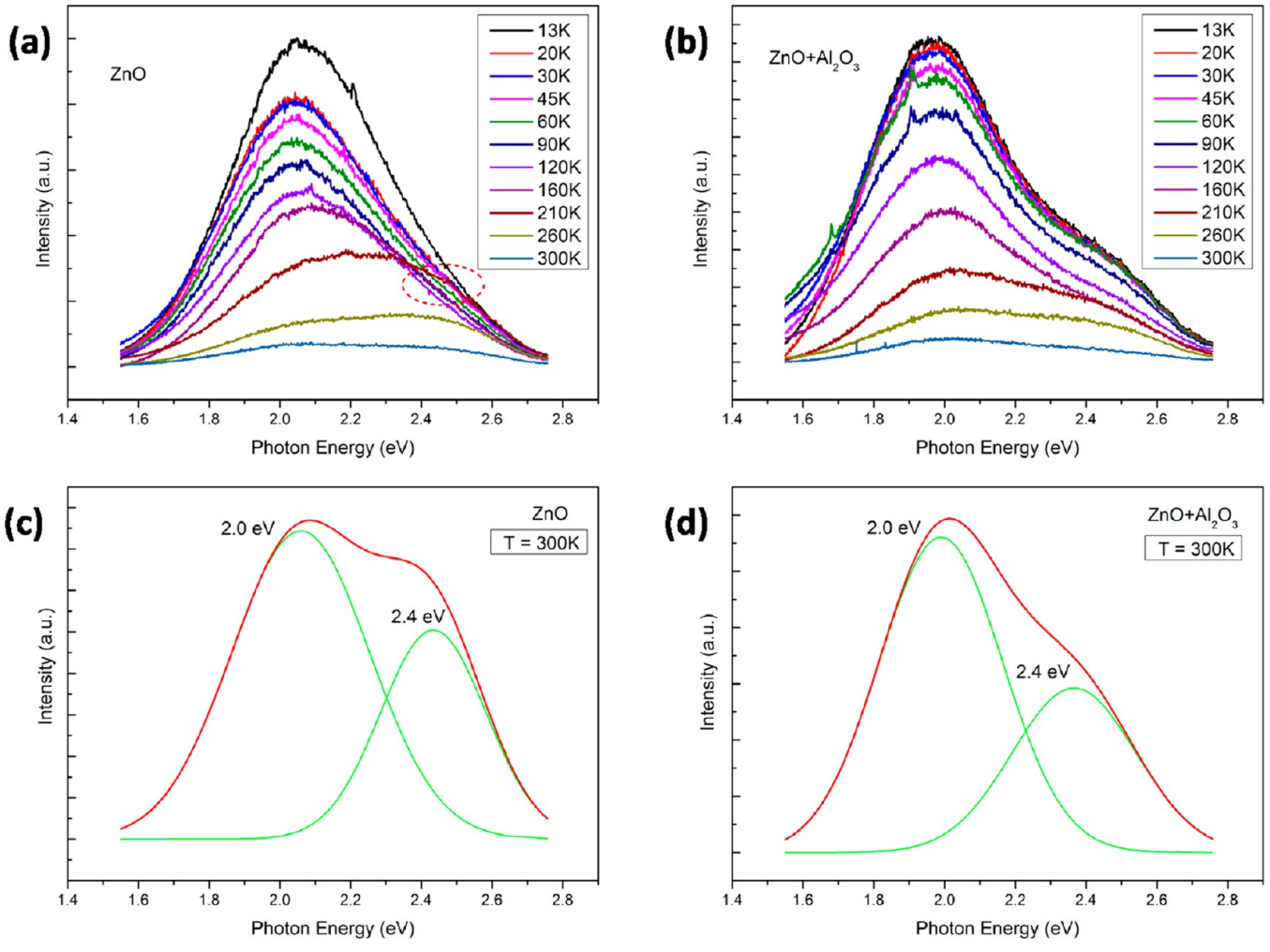

Figure 6. Temperature-dependent PL spectra of the deep level emission for the (a) as-grown and (b) Al_2O_3-coated ZnO nanorods. PL spectra (300 K) and Gaussian fit results of the deep level emission for the (c) as-grown and (d) Al_2O_3-coated ZnO nanorods.

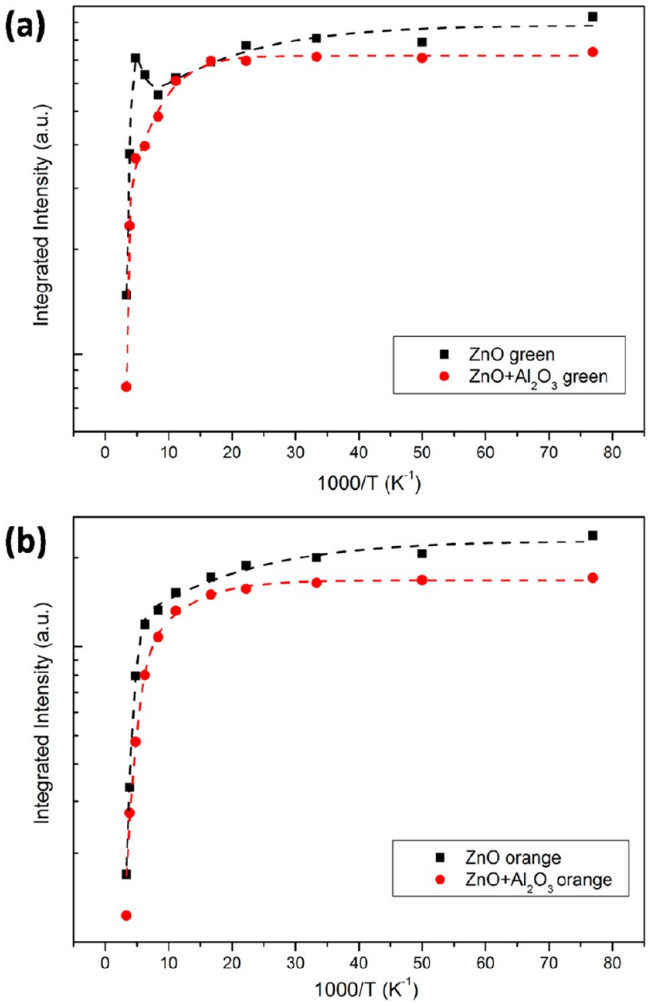

Figure 7. PL intensity of the deep level emissions as a function of reciprocal temperature for the as-grown and Al_2O_3 coated samples: (a) green emission, (b) orange emission.

lead to a low probability of radiative recombination. These holes can obtain enough thermal energy to overcome the potential barrier induced by this surface band bending.[21,22] Therefore, the PL intensity of bare ZnO will be decreased less sensitively to the increasing temperature. However, because of the Al_2O_3-coating-induced flat-band effect, fewer holes accumulate near the surface, leading to an apparent decrease in the PL intensity with increasing temperature. This phenomenon will occur when the width of the depletion region is decreased, caused by the increased electron concentration.[23] And the electron concentration can be increased by H doping through the H plasma treatment. Therefore, the PL intensities of the samples after surface treatment decayed more quickly with increasing temperature than that of the as-grown sample.

Temperature-dependent PL spectra of the deep level emissions of both the as-grown and Al_2O_3-coated ZnO nanorod arrays are plotted in panels a and b in Figure 6. It is worth mentioning that H plasma-treated sample shows negligible deep level emissions from 13 to 300 K. It can be observed that both the spectra are composed of a green emission and an orange emission from 13 to 300 K. Interestingly, the green emission of the as-grown sample shows negative thermal quenching (NTQ) behavior within a certain temperature range, as marked in the dotted region. Although this phenomenon is not observed in Al_2O_3-coated sample. The NTQ behavior that the PL intensity increases with increasing temperature within a certain temperature range has been observed in both ZnO and other semiconductors.[24−27] Some researchers have suggested that the NTQ behavior was attributed to the release of carriers/excitons from localized or trap states.[24] The visible emission at 300 K is decomposed into a green emission near 2.5 eV and an orange emission near 2.0 eV by Gaussian fitting, as shown in panels c and d in Figure 6. An apparent decline of the contribution of the green emission after Al_2O_3 coating is observed here. It can be believed that the surface states have a greater impact on the green emission compared with the orange emission. Similarly, Shalish et al.[4] have shown that the PL intensity of the green emission changed linearly with the nanowire diameter. They also proposed a model to discuss the role of surface states. Huang et al.[28] have observed the NTQ behavior of the green emission in Cu-doped ZnO nanorods and they thought that this behavior was a characteristic of Cu dopants. Considering that the NTQ behavior is disappeared after surface coating in our work, we suggest that this behavior is induced by surface states. The NTQ behavior is more clearly seen in Figure 7a, indicating that the Al_2O_3-coated sample exhibits significantly different thermal behaviors for the green emission compared with the as-grown ZnO. However, the thermal behavior of the orange emission does not change much after Al_2O_3 coating, as shown in Figure 7b. Our results prove that surface states have crucial influence on the luminescence properties of ZnO nanostructures.

CONCLUSIONS

In summary, temperature-dependent PL of the as-grown, Al_2O_3-coate,d and H plasma-treated ZnO nanorod arrays were investigated. The as-grown sample exhibits a strong near band emission and a visible emission which can be decomposed into a green emission and an orange emission. The deep level emissions are reduced after Al_2O_3 coating, whereas the NBE is little affected. H plasma treatment completely quenches the deep level emissions and enhances the NBE by ~100 times. The phenomenon observed here can be explained by surface passivation effect and hydrogen doping. The passivation effect was confirmed by the changes of the O 1s and Zn 2p spectra. An apparent decline of the contribution of the green emission after Al_2O_3 coating is observed. It is concluded that surface states have a greater impact on the green emission than the orange emission and may lead to the NTQ of the green emission. The present study can promote our understanding of the impact of the optical properties of ZnO nanostructures.

AUTHOR INFORMATION

Corresponding Author

*E-mail: yflu@zju.edu.cn. Fax: +86 571 87952625. Tel: +86 571 87952625.

Author Contributions

The manuscript was written through contributions of all authors. All authors have given approval to the final version of the manuscript.

Notes

The authors declare no competing financial interest.

■ ACKNOWLEDGMENTS

This work was supported by National Basic Research Program of China under Grants 51172204, 51072181, 21003105, 51202217, and 51172203 and Doctoral Fund of Ministry of Education of China under Grants 20110101110028 and 20120101120116.

■ REFERENCES

(1) Xia, Y.; Yang, P.; Sun, Y.; Wu, Y.; Mayer, B.; Gates, B.; Yin, Y.; Kim, F.; Yan, H. *Adv. Mater.* **2003**, *15*, 353.
(2) Zhou, H. J.; Wissinger, M.; Fallert, J.; Hauschild, R.; Stelzl, F.; Klingshirn, C.; Kalt, H. *Appl. Phys. Lett.* **2007**, *91*, 181112.
(3) Wishmeier, L.; Voss, T.; Ruckmann, I.; Gutowski, J.; Mofor, A. C.; Bakin, A.; Waag, A. *Phys. Rev. B* **2006**, *74*, 195333.
(4) Shalish, I.; Temkin, H.; Narayanamurti, V. *Phys. Rev. B* **2004**, *69*, 245401.
(5) Richters, J. P.; Voss, T.; Kim, D. S.; Scholz, R.; Zacharias, M. *Nanotechnology* **2008**, *19*, 305202.
(6) Park, W. I.; Yoo, J.; Kim, D. W.; Yi, G. C.; Kim, M. *J. Phys. Chem. B* **2006**, *110*, 1516.
(7) Lin, C. C.; Chen, H. P.; Liao, H. C.; Chen, S. Y. *Appl. Phys. Lett.* **2005**, *86*, 183103.
(8) Liu, K. W.; Chen, R.; Xing, G. Z.; Wu, T.; Sun, H. D. *Appl. Phys. Lett.* **2010**, *96*, 023111.
(9) Chen, R.; Ye, Q. L.; He, T. C.; Wu, T.; Sun, H. D. *Appl. Phys. Lett.* **2011**, *98*, 241916.
(10) Ozgur, U.; Alivov, Y. I.; Liu, C.; Teke, A.; Reshchikov, M. A.; Dogan, S.; Avrutin, V.; Cho, S. J.; Morkoc, H. *J. Appl. Phys.* **2005**, *98*, 041301.
(11) Garces, N. Y.; Wang, L.; Bai, L.; Giles, N. C.; Halliburton, L. E.; Cantwell, G. *Appl. Phys. Lett.* **2002**, *81*, 622.
(12) Yang, Y.; Tay, B. K.; Sun, X. W.; Sze, J. Y.; Han, Z. J.; Wang, J. X.; Zhang, X. H.; Li, Y. B.; Zhang, S. *Appl. Phys. Lett.* **2007**, *91*, 071921.
(13) Kim, W.; Kwak, G.; Jung, M.; Jo, S. K.; Miller, J. B.; Gellman, A. J.; Yong, K. J. *J. Phys. Chem.C* **2012**, *116*, 16093.
(14) Dev, A.; Niepelt, R.; Richters, J. P.; Ronning, C.; Voss, T. *Nanotechnology* **2010**, *21*, 065709.
(15) Huang, X. H.; Tay, C. B.; Zhan, Z. Y.; Zhang, C.; Zheng, L. X.; Venkatesan, T.; Chua, S. J. *CrystEngComm* **2011**, *13*, 7032.
(16) Huang, X. H.; Zhan, Z. Y.; Pramoda, K. P.; Zhang, C.; Zheng, L. X; Chua, S. J. *CrystEngComm* **2012**, *14*, 5163.
(17) Chen, M.; Wang, X.; Yu, Y. H.; Pei, Z. L.; Bai, X. D.; Sun, C.; Huang, R. F.; Wen, L. S. *Appl. Surf. Sci.* **2000**, *158*, 134.
(18) Yadav, H. K.; Screenivas, K.; Gupta, V.; Singh, S. P.; Katiyar, R. S. *J. Mater. Res.* **2007**, *22*, 2404.
(19) Cox, S. F. J.; Davis, E. A.; Cottrell, S. P.; King, P. J. C.; Lord, J. S.; Gil, J. M.; Alberto, H. V.; Vilao, R. C.; Duarte, J. P.; de Campos, N. A.; Weidinger, A.; Lichti, R. L.; Irvine, S. J. C. *Phys. Rev. Lett.* **2001**, *86*, 2601.
(20) Meyer, B. K.; Alves, H.; Holfmann, D. M.; Kriegseis, W.; Forster, D.; Bertram, F.; Christen, J.; Hoffmann, A.; Straßburg, M.; Dworzak, M.; Haboeck, U.; Rodina, A. V. *Phys. Stat. Sol. (b)* **2004**, *241*, 232.
(21) Yang, W. C.; Wang, C. W.; He, J. H.; Chang, Y. C.; Wang, J. C.; Chen, L. J.; Chen, H. Y.; Gwo, S. *Phys. Stat. Sol. (a)* **2008**, *205*, 1190.
(22) Chen, C. Y.; Lin, C. A.; Chen, M. J.; Lin, G. R.; He, J. H. *Nanotechnology* **2009**, *20*, 185605.
(23) Seró, I. V.; Santiago, F. F.; Denier, B.; Bisquert, J.; Zaera, R. T.; Elias, J.; Clément, C. L. *Appl. Phys. Lett.* **2006**, *89*, 203117.
(24) Shibata, H. *Jpn. J. Appl. Phys.* **1998**, *37*, 550.
(25) Watanabe, M.; Sakai, M.; Shibata, H.; Satou, C.; Shibayama, T.; Tampo, H.; Yamada, A.; Matsubara, K.; Sakurai, K.; Ishizuka, S.; Niki, S.; Maeda, K.; Niikura, I. *Physica B* **2007**, *376*, 711.
(26) Hauser, M.; Heping, A.; Hauschild, R.; Zhou, H. J.; Fallert, J.; Kalt, H.; Klingshirn, C. *Appl. Phys. Lett.* **2008**, *92*, 211105.
(27) He, H. P.; Wang, Y. J.; Wang, J. R.; Ye, Z. Z. *Phys. Chem. Chem. Phys.* **2011**, *13*, 14902.
(28) Huang, X. H.; Zhang, C.; Tay, C. B.; Venkatesan, T.; Chua, S. J. *Appl. Phys. Lett.* **2013**, *102*, 111106.